The effect of low concentrations of CO on H_2 adsorption and activation on Pt/C. Part 1: In the absence of humidity

Jack Z. Zhang [a], Zhiming Liu [a,b], James G. Goodwin Jr. [a,*]

[a] *Department of Chemical and Biomolecular Engineering, Clemson University, 127 Earle Hall, Clemson, SC 29634-0909, USA*
[b] *State Key Laboratory of Chemical Resource Engineering, Beijing University of Chemical Technology, Beijing 100029, China*

ARTICLE INFO

ABSTRACT

The presence of CO in the H_2-rich gas used as fuel for hydrogen fuel cells has a detrimental effect on PEMFC performance and durability at conventional operating conditions. This paper reports on an investigation of the effect of CO on H_2 activation on a fuel cell Pt/C catalyst close to typical PEMFC operating conditions using H_2–D_2 exchange as a probe reaction and to measure hydrogen surface coverage. While normally limited by equilibrium in the absence of impurities on Pt at typical fuel cell operating temperatures, the presence of ppm concentrations of CO increased the apparent activation energy (E_a) of H_2–D_2 exchange reaction (representing H_2 activation) from approximately 4.5–5.3 kcal mole^{-1} (Bernasek and Somorjai (1975) [24], Montano et al. (2006) [25]) (in the absence of CO) to 19.3–19.7 kcal mole^{-1} (in the presence of 10–70 ppm CO), similar to those reported by Montano et al. (2006) [25]. Calculations based on measurements indicate a CO surface coverage of approximately 0.55 ML at 80 °C in H_2 with 70 ppm CO, which coincide very well with surface science results reported by Longwitz et al. (2004) [5]. In addition, surface coverages of hydrogen in the presence of CO suggest a limiting effect on hydrogen spillover by CO. Regeneration of Pt/C at 80 °C in H_2 after CO exposure showed only a partial recovery of Pt sites. However, enough CO-free Pt sites existed to easily achieve equilibrium conversion for H_2–D_2 exchange. This paper establishes the baseline and methodology for a series of future studies where the additional effects of Nafion and humidity will be investigated.

© 2010 Elsevier B.V. All rights reserved.

1. Introduction

Today, with potential global warming and shrinking sources of liquid fossil fuels, applications for proton exchange membrane fuel cells (PEMFCs) have broadened to the automotive industry due to their advantageous characteristics such as high current density, quick startup, and zero polluting emissions [1]. However, due to the typical low temperature of operation (ca. 80 °C) and the choice of Pt as the electrocatalyst, the detrimental effects that impurities, especially CO from H_2 production via hydrocarbon reforming, have on the durability and performance of PEMFCs are some of the greatest impediments to their successful commercialization [2].

Depending on the Pt-loading in the electrode, studies show CO tolerances from 2 to 5 ppm for low Pt-loadings to as high as 20 ppm at higher Pt-loadings [3]. Modifications of the Pt electrode, such as alloying with Ru, have supposedly increased CO tolerances up to as much as 100 ppm [3]. In one report, continuous exposure to 50 ppm of CO for 6 h yielded less than a 3% voltage decrease in

PEMFC performance while exposure to 70 ppm of CO for 6 h caused an 85% voltage drop [4].

While the poisoning effect that CO has on PEMFC performance is well documented, there exists differing opinions between the surface science and electrochemical communities regarding the extent and fundamental characteristics of this poisoning. For example, results from high pressure scanning tunneling microscopy (HP STM) and density functional theory (DFT) calculations of adsorption of CO on Pt(1 1 1) over the pressure range (P_{CO}) of 10^{-6} to 760 Torr at room temperature show an increase in the ratio of amount of surface CO to Pt_S (CO/Pt_S), where Pt_S indicates exposed surface atoms of Pt, from 0.5 to 0.7 [5–7]. While the authors related this ratio to the surface coverage of Pt_S by CO, the ambiguity in their definition of "surface coverage" and the lack of information accounting for bridge-bonded CO, where one molecule of CO occupies two Pt_S atoms, makes it uncertain whether the fraction of Pt_S surface covered by CO was 0.7 or 1.0. It is important to note that this CO/Pt_S ratio was also obtained in the absence of H_2. In contrast, electrochemical results on Pt electrodes via cyclic voltammetry (CV) suggest a completely covered Pt surface ($\theta_{CO/Pt}$ = 1) at much lower CO concentrations of 100 ppm CO in the presence of H_2 [8,9]. However, calculation of surface coverage based on CV measurement of peak currents is imprecise and is not an ideal quantitative technique

* Corresponding author. Tel.: +1 864 6656 6614; fax: +1 864 656 0784.
E-mail address: jgoodwi@clemson.edu (J.G. Goodwin Jr.).

[10]. While discrepancies between these results may be attributed to differences in experimental conditions and methods of measurement, Longwitz et al. [5] also pointed out that extreme care must be taken when relating UHV results to systems operating under realistic conditions, such as at atmospheric pressure.

Due to the number of ambiguities regarding CO poisoning on Pt, such as the ones outlined above, research was carried out to investigate the fundamental effect of CO on H_2 activation on a commercial Pt/C catalyst used in fuel cells. This effect was studied utilizing H_2–D_2 exchange (as a probe reaction related to hydrogen activation) and surface concentration measurements of hydrogen and CO at conventional PEMFC operating conditions (80 °C, 2 atm) and in the absence of humidity. While the presence of humidity would have a notable effect on the adsorption of CO on Pt, as shown qualitatively via ATR-IR and Raman spectroscopy by Ebbesen et al. [11] and Ren et al. [12], respectively, quantitative measurement of CO surface coverage on Pt using the proposed new methodology involving H_2–D_2 must first be established in the absence of humidity before the additional effects of Nafion and water can be investigated. In addition, measurements in the absence of water vapor permit a more direct comparison of results concerning CO and hydrogen coverages on Pt/C at typical fuel cell conditions to results on this topic for single crystal surfaces of Pt in the surface science literature. Comparison and verification of the exchange reaction as a valid test reaction for the electrocatalytic oxidation of H_2 on Pt can be found elsewhere [13].

2. Experimental

2.1. Catalyst characterization

A commercial Pt fuel cell catalyst, 20 wt% Pt supported on carbon black (Vulcan XC-72, Cabot Co.) (Pt/C), was purchased from BASF. Nominal composition was confirmed via elemental analysis (performed by Galbraith Laboratories) and energy dispersive X-ray spectroscopy (EDX) (STEM-Hitachi HD2000 equipped with an Oxford INCA Energy 200 EDS).

BET surface area, pore size, and pore volume measurements were carried out with a Micromeritics ASAP 2020. Samples of Pt/C were degassed under vacuum (10^{-3} mm Hg) at 100 °C for 3 h prior to analysis. Results were obtained from N_2 adsorption isotherms at −196 °C.

H_2 and CO chemisorption experiments were performed at various analysis temperatures (35 and 80 °C) in a Micromeritics ASAP 2010 equipped with a chemisorption controller station. Samples were pretreated in flowing H_2 at 80 °C for 3 h prior to analysis. Due to the presence of Nafion in the catalyst layer in a fuel cell, a low pretreatment temperature is necessary because of the thermal limitations of the Nafion. However, temperature programmed reduction (TPR) of Pt/C showed the catalyst to be fully reduced under the pretreatment conditions employed. After pretreatment, samples were evacuated (10^{-5} mm Hg) at 80 °C for 3 h prior to analysis. The temperature was then adjusted to the specified analysis temperature and the H_2 or CO isotherms were obtained from 50 to 450 mm Hg at increments of 50 mm Hg. Volumetric uptakes of CO or H_2 were used to determine total number of surface Pt atoms and metal dispersion by assuming stoichiometric ratios of 1:1 for CO:Pt_S and H:Pt_S. Average Pt particle size based on chemisorption results was calculated from Eq. (1) [14]:

$$\text{average Pt particle size (nm)} = \frac{1.08}{\text{metal dispersion}} \qquad (1)$$

Transmission electron microscopy (TEM) images and EDX spectra were obtained using a STEM-Hitachi HD2000 analytical electron microscope. Samples for TEM imaging were prepared by suspending small amounts of the catalyst in isopropyl alcohol and agitating

in a sonicator until an even dispersion of catalyst was observed. A small drop of the dispersed sample was then transferred onto a copper grid. Sample grids were then allowed to dry at room temperature overnight prior to measurement. Approximate average Pt particle size of the catalyst was obtained by averaging diameters of 100+ particles from the TEM images. The result was further confirmed via X-ray diffraction (XRD) (Scintag XDS 2000 powder diffractometer equipped with Cu Kα radiation) on as-received and reduced (80 °C in H_2 for 3 h) then passivated Pt/C with a scanning range from 20° to 85° and a step-size of 0.02° min^{-1}.

Diffuse reflectance FT-IR measurements were carried out in a Nicolet 6700 FTIR spectrometer equipped with a Harrick diffuse reflectance infrared Fourier transform (DRIFT) cell fitted with ZnSe windows. The DRIFTS study of Pt/C was complicated by the carbon support which is a strong absorber of the IR beam. In order to get a detectable signal, the Pt/C catalyst was mixed with KBr powder at a ratio of Pt/C:KBr = 1:100. The feed flow rate was fixed at 50 sccm. Prior to exposure to CO, the catalyst was pretreated *in situ* at 350 °C in a flow of H_2 for 1 h, followed by flushing with He for 30 min, and then cooled to the desired temperature for taking a reference spectrum. The higher pretreatment temperature of 350 °C was used to ensure a clean Pt surface prior to the introduction of CO. As mentioned above, this high of a pretreatment temperature of Pt/C would not be possible for Nafion–Pt/C since degradation of Nafion occurs at temperatures higher than 120 °C. However, for the purposes here, there is minimal difference in Pt/C reduced at 80 or 350 °C. FT-IR spectra of CO adsorption on Pt/Al_2O_3 [15,16] showed pretreatment temperature to have a negligible effect on band frequency.

After taking a reference spectrum, a gas mixture of 4% CO in H_2 (or pure CO) was fed to the reduced catalyst for 1 h, followed by flushing with He for 10 min prior to taking the spectra. All spectra reported here were taken at a resolution of 4 cm^{-1}. Interpretation of FT-IR results is limited qualitatively to the surface species present after the introduction of CO.

2.2. H_2–D_2 exchange reaction

Experiments were performed in a conventional plug flow, micro-reactor system pressurized at 2 atm (Fig. 1). All gases were purchased from Scott specialty gases with research grade purity. Similar to chemisorption, prior to reaction experiments, all catalyst samples were pretreated at 80 °C in H_2 for 3 h. Measurements of the apparent activation energies (E_a) were obtained with catalyst samples of 10 mg of Pt/C mixed with 40 mg of XC-72 to achieve differential reaction conditions. Temperature for apparent E_a measurements was varied from 50 to 90 °C.

While the anodic feed stream for PEMFCs is primarily H_2, the use of Ar was required in this study, primarily for purging the system when measuring hydrogen surface concentration, see Section 2.3. For calibration purposes, in order to maintain a relatively constant pressure inside the MS, the reactant mixture for the exchange reaction was also diluted with Ar. The effluent gas (comprised of H_2, D_2, Ar, and HD) was analyzed with a Pfeiffer Vacuum MS. Reactions in the absence of CO were performed by flowing 100 sccm of 20% H_2, 20% D_2, and 60% Ar through the catalyst bed. For experiments involving CO, the impurity concentration was varied by mixing flows of 500 ppm CO in H_2 with pure H_2 and keeping the same overall reaction mixture as above. The exchange conversion was obtained via Eq. (2) using the H_2 ($m/z = 2$) and D_2 ($m/z = 4$) MS signals in the presence and absence of catalyst:

$$\text{conversion (\%)} = \frac{(H_2 \text{ or } D_2 \text{ signal})_{\text{no Cat.}} - (H_2 \text{ or } D_2 \text{ signal})_{\text{Cat.}}}{(H_2 \text{ or } D_2 \text{ signal})_{\text{no Cat.}}} \qquad (2)$$

Except for time-on-stream (TOS) experiments, exchange results in the presence of CO were obtained at CO adsorption/desorption
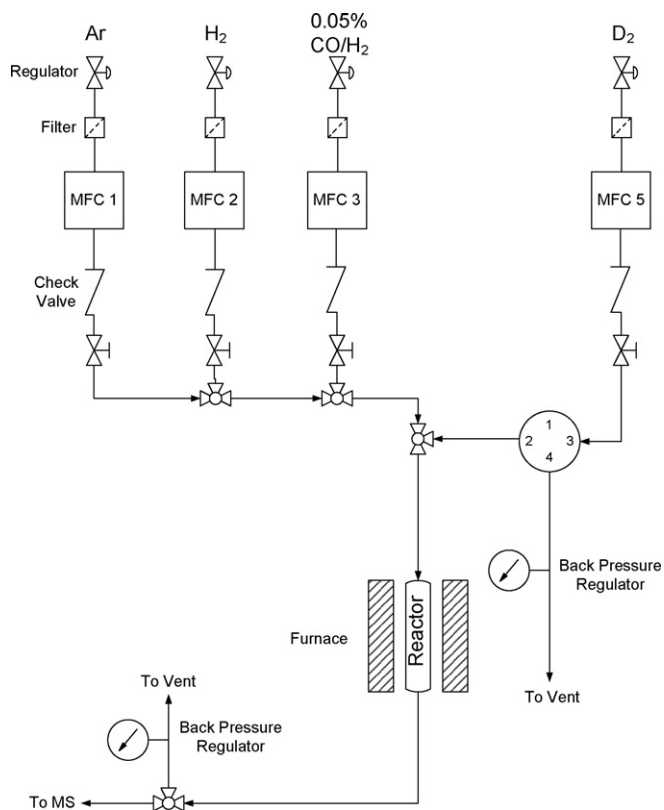
Fig. 1. Flow apparatus used for H_2–D_2 exchange, HDSAP, and TPD measurements.

equilibrium such that no further change in HD signal was observed (steady-state).

2.3. H_2–D_2 switch with Ar purge (HDSAP)

Because the H_2–D_2 exchange reaction is always able to reach equilibrium in the absence of CO under the specified experimental conditions for even small amounts of catalyst (~1 mg), it cannot be used as a baseline in determining the degree of CO poisoning on the Pt/C catalyst. Instead, a better method of comparison had to be developed by measuring the surface concentration of hydrogen in the absence and presence of CO. Although temperature programmed desorption (TPD) can essentially provide a similar type of measurement, the high temperatures involved normally in TPD greatly alters the physical characteristics of the catalyst and could only be performed at the very end of an experiment. On the other hand, H_2–D_2 switch with an Ar purge (HDSAP) provided a non-destructive measurement that could be performed at any point during a particular experiment. Agreement of surface concentration of hydrogen measurements obtained from HDSAP with those from static H_2 chemisorption was found for the Pt/C catalyst (as shown later).

Due to the high porosity of XC-72 (S_{BET} = 218 m^2 g^{-1}), high concentration of Pt (20 wt% Pt/C), and the extremely fast rate of the exchange reaction, when a switch from H_2 is made directly to D_2 in the reactor, some of the gas-phase H_2 in the catalyst pores is still able to dissociate on the Pt particles and react with adsorbed deuterium atoms before it can diffuse out of the pores. The resulting estimation of hydrogen surface concentration from the amount of HD and H_2 formed would, thus, be a combination of both gas-phase H_2 inside the pores and surface hydrogen atoms at the time of the switch and, therefore, would be an over estimation of the desired quantity. A solution to this problem was arrived at by the addition of purging with an inert gas (Ar) between the switch from H_2 to D_2.

HDSAP measurements were initiated by flowing a gas mixture comprised of 20% H_2 and 80% Ar (total = 100 sccm) for 30 min. The H_2 was then turned off and 80 sccm of Ar was passed through the reactor for 30 min (purge period). This was done to purge as much of the gas-phase or weakly adsorbed H_2 from the catalyst as possible. Preliminary HDSAP experiments showed 30 min to be optimal for both exposure and purge times for our catalyst. Once the purge was complete, a flow of 20 sccm of D_2 (along with 80 sccm of Ar) was introduced to the catalyst. Two peaks for HD and H_2 were observed in the MS after the D_2 switch. The amount of HD and H_2 were calculated by integrating the area under these peaks and using the respective areas from the exchange reaction as calibration. Total surface concentration of hydrogen was calculated from the sum of the amounts of hydrogen (H) in HD and H_2, as given by Eq. (3):

$$\text{surface H}(\mu\text{mol g Cat.}^{-1}) = \mu\text{mol HD g Cat.}^{-1}$$

$$+ 2 \times \mu\text{mol H}_2 \text{ g Cat.}^{-1} \tag{3}$$

Validation of this technique is given in Section 3.

Due to the high detection limit of mass spectrometers (MS), measurements of hydrogen surface concentrations were performed on catalyst samples of 100 mg Pt/C. This did not present a problem since equilibrium surface concentration was being measured and not rates of adsorption/desorption.

2.4. TPD

For measurements of CO surface concentration at steady-state, TPD measurements were performed at the end of each experiment. After the last HDSAP measurement, flow was switched to 20 sccm Ar and allowed to stabilize for 10 min. Due to the possibility of some CO desorbing, the temperature was ramped directly from 80 to 600 °C, instead of cooling to 35 °C, at a rate of 10 °C min^{-1} while following, via the MS, CO and other possible carbonaceous species (CH_4 and CO_2) desorbing. The latter two species were recorded in case that, at the higher temperatures during the ramp, CO reaction with surface H or O (from another CO) was able to occur. These signals were compared to TPD spectra of Pt/C not exposed to CO.

3. Results and discussion

3.1. Catalyst characterization

3.1.1. BET

BET surface area, pore size, and pore volume were 225 ± 12 m^2 g^{-1}, 16.4 ± 1.8 nm, and 0.63 ± 0.04 cm^3 g^{-1} for the carbon support (XC-72), respectively; and 186 ± 5.6 m^2 g^{-1}, 19.7 ± 4.2 nm, and 0.57 ± 0.01 cm^3 g^{-1} for Pt/C, respectively. Results for XC-72 correspond well to values in the literature [17,18]. While little change was observed for pore size and volume, the addition of Pt to the carbon support reduced the BET surface area by ca. 17%.

3.1.2. Average particle size (TEM and XRD)

Analysis of TEM images indicated a fairly even distribution of Pt particles on XC-72 in the Pt/C catalyst (Fig. 2). Average Pt particle size for the as-received Pt/C was determined to be 4.0 ± 0.9 nm. Exposure of Pt/C to H_2 and H_2/Ar at 80 °C for 24 h had no effect on its average particle size, suggesting that the sintering process is very slow at 80 °C. Similar results were obtained via XRD using the Debye–Scherrer equation and the full width at half maximum (FWHM) of the Pt(1 1 1) diffraction peak for both the as-received and pretreated Pt/C (ca. 3 and 4 nm, respectively) (Fig. 3). From left to right, 2θ values of 25°, 40°, 45°, 68°, and 81° in Fig. 3 correspond to diffractions of graphite (0 0 2), Pt(1 1 1), Pt(2 0 0), Pt(2 2 0), and Pt(3 1 1), respectively [19,20]. The difference between the two val-
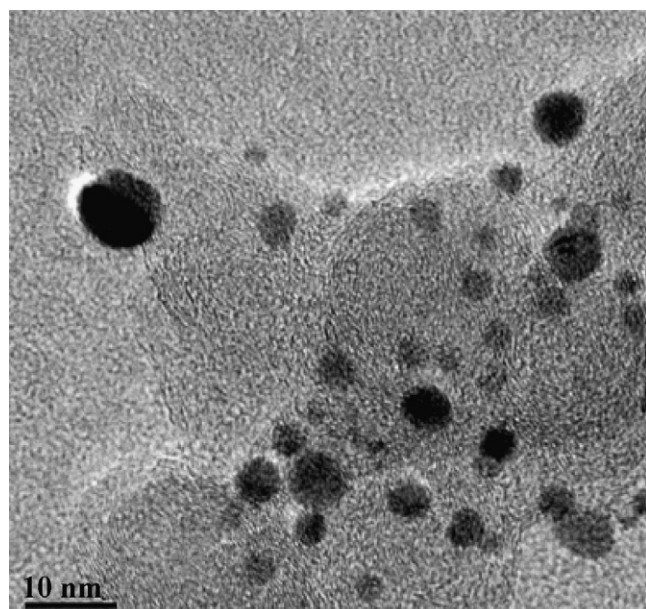
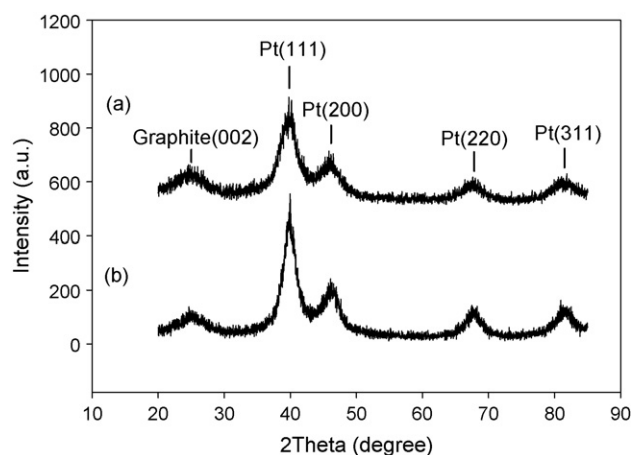**Fig. 2.** TEM image of as-received 20 wt% Pt/C.

Fig. 3. XRD spectra of Pt/C (a) as-received and (b) pretreated in H_2 at 80 °C.

ues of the average Pt particle size determined by XRD relates to the reduction of the oxide layer surrounding the metal particles during pretreatment. Thus, results from both TEM and XRD appear to suggest an average Pt particle size of approximately 4 nm for this catalyst when reduced.

3.1.3. Elemental analysis

Elemental analysis results for Pt/C from Galbraith Laboratories and EDX showed a Pt-loading of 19.2 wt% as well as a large amount of sulfur (~0.4 wt%). Similar amounts of sulfur were obtained from analysis results for the carbon support (XC-72) itself. Most likely,
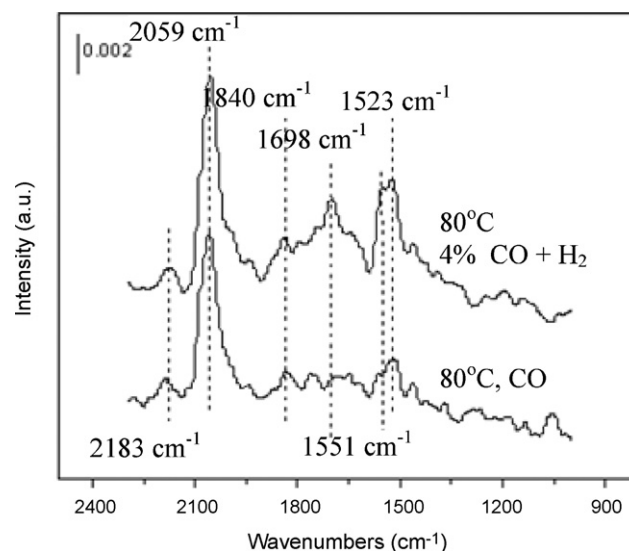

Fig. 4. DRIFTS-FTIR spectra of 20 wt% Pt/C at 80 °C after exposure to 4% CO + H_2 and 100% CO.

this sulfur was due to the vulcanization process used in producing the activated carbon support. It is important to note that, although sulfur helps in dispersing Pt particles during impregnation, extended runs in PEMFCs showed faster degradation of fuel cell performance when sulfur-containing carbon supports were used [17,21,22]. However, due to the low temperature used in this investigation and the short experimental times, compared to the extended fuel cell runs, the sulfur present in the carbon support should have had a minimal effect.

3.1.4. Static H_2 and CO chemisorption

Regardless of analysis temperature (35–80 °C), the amount of CO uptake remained relatively constant (Table 1). This suggests that CO does not spill over onto the carbon support. Average Pt particle size calculated from CO chemisorption is higher than that from the TEM images; the difference in the results is due to the existence of linear and bridge-bonded CO on Pt, such that the overall stoichiometry CO:Pt_S is actually <1. Results from DRIFTS-FTIR experiments (Fig. 4) exposing Pt/C at 80 °C to 4% CO in H_2 and pure CO show the existence of linear-bonded and some bridge-bonded CO at 2059 and 1840 cm^{-1} wavenumbers, respectively. Evidence of CHx species (wavenumber 1523 cm^{-1}) present on the Pt surface is also apparent. However, TPD results showed little or no desorption of CH_4 during the temperature ramp.

Contrary to CO chemisorption results, depending on the analysis temperature (35 °C vs. 80 °C), the amount of H_2 uptake during H_2 chemisorption varied from 215 to 255 μmol H g cat^{-1}, respectively. Although both concentrations yield average Pt particle sizes (4.2–4.9 nm, Eq. (1)) within the range observed by TEM, the former is closer to the estimated average size. Thus, due to the probability of H_2 spillover at higher temperatures, especially on a

Table 1
Static H_2 and CO chemisorption results at 35 and 80 °C for 20 wt% Pt/C[a].

Adsorption gas	Analysis temp. (°C)	Amount of CO/H adsorbed[b] (μmol g cat^{-1})	Metal dispersion (%)	Avg. Pt particle size (nm)[c]
CO	35	190	19	5.7
	80	200	20	5.4
H_2	35	215	22	4.9
	80	255	26	4.2

[a] Pt/C was pretreated in H_2 at 80 °C for 3 h.
[b] Experimental error for all results was ca.±3%.
[c] Avg. Pt particle size calculated from Eq. (1) assuming CO/Pt_S = 1 and H/Pt_S = 1.

Table 2
Effect of Ar and time, in the absence of CO, on total surface concentration of hydrogen on Pt/C[a] from HDSAP.

Exposure gas[b]	Surface H concentration (μmol g cat^{-1})[c]		
	After pre-treatment	12 h of exposure	24 h of exposure
H$_2$ only	284	271	273
20 H$_2$/80 Ar mixture	291	265	265

[a] Pt/C was pretreated at 80 °C in H$_2$ for 3 h.
[b] Total pressure = 2 atm.
[c] Experimental error for all results was ca. ±8%.

carbon support [23], and considering the CO chemisorption results, the actual concentration of surface Pt atoms on Pt/C is estimated to be approximately 215 μmol H g cat^{-1}. The additional 40 μmol H g cat^{-1} uptake at 80 °C is likely due to hydrogen spillover.

3.1.5. Validation of H$_2$ surface concentration results from HDSAP

While Ar itself is inert, due to its employment as a diluent in HDSAP, its effect or lack thereof on hydrogen surface concentration should be established. In addition, any difference in hydrogen surface coverage with H$_2$ partial pressure between that of these studies (0.4 atm) and those of typical fuel cells (1–2 atm) must be addressed. This comparison was carried out by exposure of Pt/C to a gas mixture of (20/80) H$_2$/Ar (2 atm total pressure) for an extended period of time (24 h). The same procedure was performed for Pt/C exposed to pure H$_2$ (2 atm). The results (Table 2) suggest that the dilution of the feed stream by Ar and a variation in the partial pressure of H$_2$ (0.4–2 atm) has a minimal effect on the concentration of hydrogen on Pt/C.

The hydrogen surface concentrations based on HDSAP, after both 12 and 24 h of exposure to either H$_2$ or H$_2$/Ar, in the absence of CO appear to be within experimental error of that of static H$_2$ chemisorption at 80 °C (Table 1). The slightly higher surface concentration of hydrogen from HDSAP, obtained immediately after pretreatment, may be due to surface functional groups on the carbon support, leftover from the impregnation process to achieve higher Pt dispersion [17]. Extended exposure to H$_2$ appeared to stabilize the concentration of hydrogen adsorbed on the catalyst. It is also important to note that, while the hydrogen surface concentration is able to be obtained by HDSAP immediately after pretreatment, the time required for complete chemisorption analysis is approximately 12 h under the conditions employed. Thus, accounting for these factors, the hydrogen surface concentrations obtained from HDSAP at 80 °C in flow and from static chemisorption at 80 °C appear to be the same. Therefore, HDSAP appears to be an excellent experimental method for the measurement of hydrogen surface concentration on Pt/C.

3.2. H$_2$–D$_2$ exchange reaction

In the absence of CO or other impurities, the exchange reaction is equilibrium limited on even small quantities of Pt catalyst,
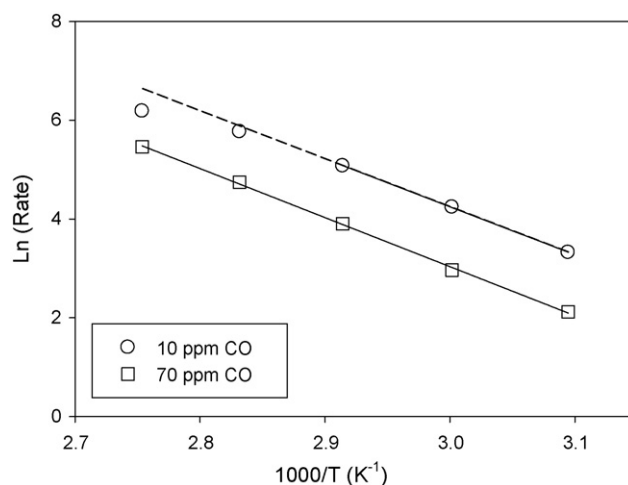

Fig. 5. Apparent activation energy of H$_2$–D$_2$ exchange on Pt/C in the presence of 10 and 70 ppm of CO. All reaction rates were obtained at steady-state for % H$_2$–D$_2$ conversion.

even at 35 °C. For this reason, in the absence of impurities, the hydrogen oxidation reaction (HOR, H$_2 \leftrightarrow 2H^+ + 2e^-$) is rarely the rate-limiting step in fuel cell operation, even at high current densities [3]. Such was the case here even using 0.5 mg of Pt/C for the conditions employed. For an equal molar flow of H$_2$ and D$_2$ at 80 °C, equilibrium is approximately 45% conversion of H$_2$.

As will be shown later, the steady-state coverage of Pt$_S$ by CO is not 100%, even at as high as 200 ppm CO, under the experimental conditions employed. This partial coverage allows H$_2$ activation (H$_2$–D$_2$ exchange) to occur on Pt$_S$ unoccupied by CO. Thus, the effect of CO poisoning is a function of both CO concentration and amount of Pt/C, such that, even at high CO concentrations, if sufficient unoccupied-Pt$_S$ sites are available, steady-state H$_2$–D$_2$ exchange conversion could be at equilibrium. Because of this and the differential conversion condition necessary to provide a good estimation of the apparent activation energy, E_a, small amounts of Pt/C (10 mg) was mixed with carbon support (XC-72) to obtain a catalytic bed length of ca. 1 cm and to allow an even dispersion of Pt/C. The carbon support did not appear to affect the reaction as preliminary experiments of Pt/C mixed with α-Al$_2$O$_3$ showed similar results. The steady-state H$_2$–D$_2$ exchange conversion and rate were obtained for 10 and 70 ppm CO. These data are tabulated in Table 3 and shown in an Arrhenius plot (Fig. 5). It should be noted that, the steady-state H$_2$–D$_2$ exchange conversion for 10 ppm CO at 80–90 °C was significantly greater than differential conditions ($\leq$10%), and these points can be concluded to have deviated somewhat from the linear relationship with the data at lower temperatures.

The E_a in the absence of CO was not able to be obtained due to the reaction being limited by equilibrium at the experimental conditions used in this study, even for extremely small amounts of catalyst (ca. 0.5 mg). However, surface science studies of H$_2$–D$_2$

Table 3
Steady-state H$_2$–D$_2$ exchange conversion and rate on Pt/C in the presence of 10 and 70 ppm CO[a].

T (°C)	10 ppm CO		70 ppm CO	
	H$_2$–D$_2$ exchange conversion (%)[b]	Rate (μmol g^{-1} s^{-1})	H$_2$–D$_2$ exchange conversion (%)[b]	Rate (μmol g^{-1} s^{-1})
90	35.6	486.5	17.2	234.9
80	23.4	320.4	8.4	115.0
70	11.7	160.3	3.6	49.6
60	5.1	69.4	1.4	19.4
50	2.0	27.8	0.6	8.3

[a] 10 mg Pt/C at 80 °C in a H$_2$/D$_2$/Ar mixture at 2 atm with H$_2$:D$_2$ = 1, P_{Ar} = 1.6 atm.
[b] Experimental error for all results was ca. ±5%.

exchange on Pt(1 1 1) [24,25] have reported apparent E_a of 4.5 and 5.3 kcal mole^{-1} between a temperature range of 25 and 300 °C using molecular beam and low pressure experiments, respectively. However, it should be noted that these measurements may still be equilibrium affected, even at these conditions. Closer inspection of the Arrhenius plot given in Ref. [25] reveals slight curvature in both the H_2–D_2 exchange data taken in the absence and in the presence of CO. Thus, because the exchange reaction is so fast, one has to be extra cautious when interpreting these results.

Introduction of even 10 ppm CO significantly increased the apparent activation energy of the exchange reaction in the surface science studies. In the present study, values for E_a of 19.3 and 19.7 kcal mol^{-1} were measured for Pt/C in the presence of 10 and 70 ppm CO (Fig. 5), respectively. These results agree well with the value measured by Montano et al. [25] of 17.4 kcal mol^{-1} (200 mTorr H_2, 20 mTorr D_2, 5 mTorr CO) on Pt(1 1 1), overlooking the slight potential curvature of their Arrhenius plot.

Comparison of activation energies obtained for the CO poisoning of ethylene hydrogenation on Pt(1 1 1) (9.6 kcal mole^{-1} in the absence of CO and 20.2 kcal mol^{-1} in the presence of CO), show a similar trend of increasing apparent activation energy upon CO poisoning [25]. The increase in E_a may be influenced by a restructuring of the Pt surfaces by CO [25–28], which can occur even at room temperature [26,29]. Restructuring of metal surfaces is common and occurs due to thermodynamic instabilities that arise most often when the adsorbate–substrate bonds are stronger than the bonds between the substrate atoms [30]. Scanning tunneling microscopy (STM) images of Pt(1 1 0) in the presence of CO at various temperatures indicate that the CO continuously "lifts" and roughens the Pt surface over time until the surface becomes thermodynamically stable [26]. This roughening of the Pt surface and decrease in the coordination numbers of metal atoms may perhaps inhibit formation of HD by limiting the rate of diffusion of H and D atoms on the Pt surface [25]. In addition, molecular beam studies show that the H_2–D_2 exchange reaction is structure sensitive at low pressures ($\sim$10^{-7} Torr) of H_2 and D_2 [31]. However, the authors theorized that the exchange reaction is not structure sensitive at high pressures (1 atm) due to the reaction being so fast that equilibrium is usually achieved (in the absence of an impurity). The combination of (1) blocking of Pt sites, (2) surface restructuring, and (3) structure sensitivity of H_2–D_2 exchange reaction could explain why even a small amount of CO can have such a significant effect on the apparent activation energy for H_2 activation on Pt. As shown in Fig. 5, an increase in CO concentration (70 ppm) did not seem to affect the apparent activation energy further. This suggests that an increase in CO concentration beyond 10 ppm does not affect the exchange mechanism significantly.
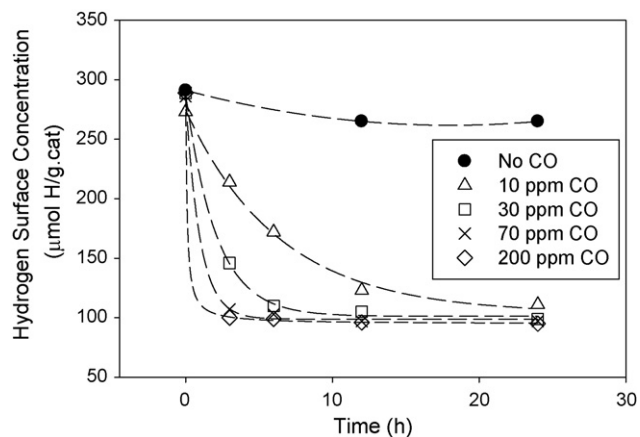

Fig. 6. TOS measurement of hydrogen surface concentration as a function of CO concentration (10–200 ppm) on Pt/C at 80 °C.

3.3. H_2 and CO surface concentration measurements

3.3.1. Effect of CO on hydrogen surface concentration

Fig. 6 shows TOS measurements of hydrogen surface concentration on 100 mg of Pt/C in the presence of 10–200 ppm CO in 20% H_2 and 80% Ar. Table 4 gives the steady-state surface concentrations. As the CO concentration increased, the time required to reach steady-state coverage decreased. This is understandable as higher CO concentrations allowed for higher initial uptakes. However, what primarily dictated the rate of decline with TOS was that, for ppm concentrations of CO, it took a long time to populate the surface of 100 mg Pt/C to steady-state coverage, even if every molecule adsorbed.

Due to adsorption/desorption equilibrium of CO at 80 °C, the surface concentration of hydrogen never approached 0 at steady-state, even in as high a concentration as 200 ppm CO. Increasing CO concentration to 200 ppm, from 70 ppm, did not appear to significantly further decrease hydrogen surface concentration or exchange conversion.

While steady-state hydrogen surface concentration is a function of CO concentration regardless of the amount of catalyst, H_2 activation or H_2–D_2 exchange conversion is not. Even though a large loss in hydrogen surface concentration was observed for 100 mg of Pt/C in the presence of 10 ppm CO, H_2–D_2 exchange at steady-state was still very close to equilibrium (ca. 42% vs. 45% at equilibrium). Exposure of 100 mg of Pt/C to 200 ppm CO further decreased H_2–D_2 exchange conversion at steady-state to 22%. This result suggests that, although CO is blocking a large portion of the sites, there are

Table 4
Steady-state H_2–D_2 exchange conversion and surface coverage of Pt/C by CO and hydrogen (from HDSAP and TPD)[a].

CO concentration (ppm)	Steady-state H_2–D_2 exchange conversion[b]	Surface H concentration at steady-state (μmol H g cat^{-1}) [HDSAP][c]	Surface CO concentration (μmol CO g cat^{-1}) [TPD][d]	Surface coverage of Pt by CO based on HDSAP (ML)[e,f]	Surface coverage of Pt by CO based on TPD (ML)[f,g]
0	45% equilibrium	265	–	–	–
2	45% equilibrium	121	51	0.44	0.24
10	42%	111	64	0.48	0.30
30	34%	99	70	0.54	0.33
70	26%	97	74	0.55	0.34
200	22%	95	72	0.56	0.33

[a] 100 mg Pt/C.
[b] Experimental error for all results was ca. ±3%.
[c] Experimental error for all results was ca. ±8%.
[d] Experimental error for all results was ca. ±5%.
[e] Calculated from Eq. (4).
[f] Calculated from Eq. (5).
[g] Calculations are based on a Pt surface concentration of 215 μmol Pt$_S$ g cat^{-1} obtained from static H_2 chemisorption at 35 °C and assuming a stoichiometry of (1:1) for both H:Pt and CO:Pt.
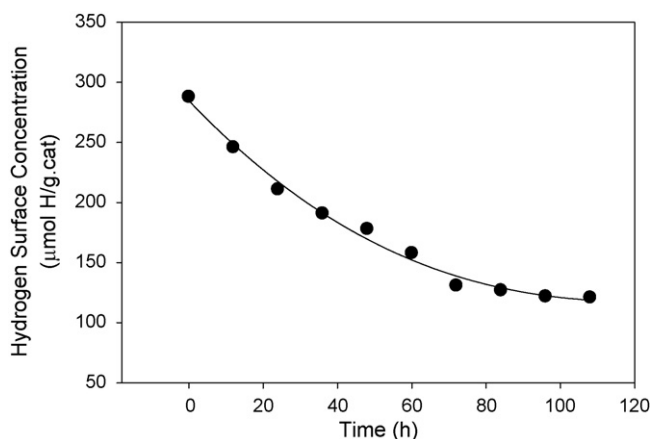
Fig. 7. Surface concentration of hydrogen on Pt/C as a function of time in the presence of 2 ppm CO.

still sufficient available Pt surface atoms remaining in the 100 mg of catalyst to cause the H_2–D_2 exchange reaction to achieve high conversions at steady-state. If, according to electrochemical results, the CO were completely covering the Pt ($\theta_{CO/Pt} = 1$) in the presence of 100 ppm CO [8,9], the steady-state conversion of H_2–D_2 exchange at 200 ppm CO should be 0%. In addition, because steady-state CO coverage on Pt_S is not 100%, even at relatively high concentrations (i.e., 200 ppm) of CO, increasing the total amount of Pt/C also increases the total number of free Pt_S sites unoccupied by CO, such that higher concentrations of CO are required before the poisoning effect can be observed. This is the reason why increasing the Pt-loading in fuel cells has the false effect of increasing its CO tolerance [3]. This is important because, regardless of how much of the Pt surface is poisoned by CO, as long as there exists enough unpoisoned Pt surface atoms such that the HOR is not the rate-limiting step, no effect of CO poisoning is observed.

Further TOS results with a lower concentration of CO (2 ppm) are shown in Fig. 7. Even after 108 h of exposure to CO, equilibrium conversion was still observed for H_2–D_2 exchange. Surprisingly, a reduction of CO from 10 to 2 ppm, which should shift the adsorption/desorption equilibrium of CO, had only a small effect on the concentration of surface hydrogen at steady-state (Table 3). Analysis of CO coverage results on Pt(1 1 1) as a function of CO pressure also showed very little change between the equivalent 2–10 ppm partial pressure range (10^{-3} to 10^{-2} Torr) [5].

3.3.2. Surface coverage of CO on Pt

Due to the ambiguity of surface coverage, the definition that will be employed in this section is based on the coverage of Pt_S by CO, such that if we have two nondissociated CO molecules bridge-bonded to four Pt_S atoms on the surface of a unit cell, we have a CO surface coverage of one monolayer ($\theta_{CO/Pt} = 1$). In other words, we are focused on surface coverage by CO as blocked surface atoms of Pt (Pt_S).

Actual surface Pt concentration is speculated to be between 190 and 215 μmol Pt_S g cat^{-1} from static CO and H_2 chemisorption results at 35 °C, respectively. The reason for this difference can be attributed to the fact that a portion of the CO is bridge-bonded to two Pt_S atoms, which is evident from IR obtained at 80 °C as well as literature [6]. Because the stoichiometric ratio of (1:1) for H:Pt_S is much more likely than that of CO:Pt_S, the Pt_S concentration of 215 μmol Pt_S g cat^{-1} obtained from static H_2 chemisorption at 35 °C was used as the basis for the surface coverage analysis. Eq. (4) was used for calculations involving hydrogen surface concentration obtained from HDSAP and Eq. (5) was used for calculations

involving CO surface concentration obtained from TPD:

CO surface coverage (HDSAP)

$$= \frac{215\ \mu mol\ Pt_S\ g\ Cat.^{-1} - (surface\ H)_{x\ ppm\ CO}}{215\ \mu mol\ Pt_S\ g\ Cat.^{-1}} \quad (4)$$

$$CO\ surface\ coverage\ (TPD) = \frac{(surface\ CO)_{x\ ppm\ CO}}{215\ \mu mol\ Pt_S\ g\ Cat.^{-1}} \quad (5)$$

These results are also tabulated in Table 4.

As expected, CO surface coverage calculated from HDSAP and TPD results both increase with CO concentration. The difference between these two results is due, in large part, to a portion of the CO being bridge-bonded such that the stoichiometric ratio of CO:Pt is less than 1. Thus, the true surface coverage of Pt_S by CO is most likely closer to the values calculated based on hydrogen surface concentration [HDSAP] than that of CO [TPD]. These results show a maximum coverage of Pt_S by CO to be approximately 0.44 ML (monolayer) and 0.56 ML for the CO concentrations of 2 and 200 ppm, respectively, at 80 °C and 0.4 atm of H_2. Further increases in CO concentration may alter CO coverage due to phenomena such as restructuring, formation of surface carbonyls, and other unforeseen variables. Furthermore, the presence of humidity may affect these results.

Considering the sum of hydrogen adsorbed (HDSAP) and the amount of CO able to be desorbed from the catalyst after exposure (TPD) and the fact that some of the CO molecules are bridge-bonded, the results from Table 4 appear to imply a limiting of hydrogen spillover by CO adsorption. In other words, the sum of 111 μmol H g cat^{-1} obtained at steady-state in 10 ppm CO (HDSAP) and the 64 μmol CO g cat^{-1} (TPD) appear to represent the surface concentration of unpoisoned and poisoned Pt_S, respectively, with the absence of hydrogen spillover. This can happen if CO is preferentially adsorbing at the outer-edges of Pt particles (i.e., Pt–C interface). Because spillover, either onto the carbon support or to the adjacent ionomer, plays an important role in proton transfer, interruption of this process can have a detrimental effect on fuel cell activity, regardless of how fast the HOR is occurring.

3.3.3. Reversibility of CO poisoning

In contrast to NH_3 on Nafion, the adsorption of CO on Pt is not permanent but rather reversible at 80 °C. This is illustrated very clearly from the adsorption/desorption equilibrium (<1 ML) that is achieved even when Pt is exposed to relatively high concentrations of CO.

From electrochemical results obtained by Uribe et al. [32], it was found that the performance of a fuel cell, previously poisoned with CO, was able to be fully regenerated within a few minutes of purging the anode with pure H_2, which appears to suggest a complete removal of adsorbed CO. Jimenez et al. [4] utilized this apparent fast reversibility of CO in a fuel cell by continuously cycling between feed streams of pure H_2 and CO/H_2 mixture every couple of minutes to improve CO tolerance. Similar to the results obtained by Uribe et al. [32], the authors also concluded that the poisoning process is reversible with only the injection of pure H_2. However, due to the high Pt-loadings (20 wt% Pt/C, 0.5 mg Pt cm^{-2}) employed and the short duration of their experiments (110 min), the system was most likely not at steady-state and would not have adsorbed enough CO to shift the HOR away from being equilibrium limited. In addition, it is again pertinent to point out that as long as there exists enough unpoisoned Pt surface atoms such that the HOR is not the rate-limiting step, no effect of CO poisoning should be observed.

Fig. 8 shows the hydrogen surface concentrations of Pt/C sequentially exposed to 30 ppm CO followed by regeneration in H_2, both for 12 h. The process was repeated a second time on the
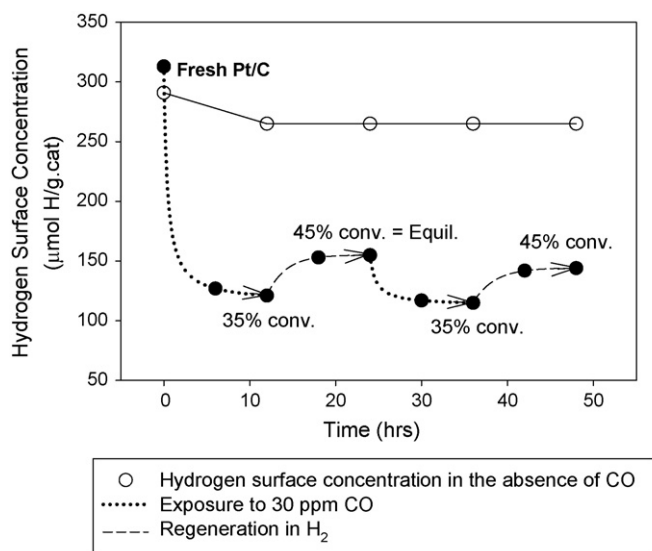
Fig. 8. Reversibility of CO poisoning after exposure of Pt/C to 30 ppm CO for 12 h. Steady-state H_2–D_2 exchange conversion was at 35% in the presence of CO and at equilibrium (~45%) for all points following regeneration.

same catalyst to see if poisoning of a previously poisoned Pt surface would yield different results. After an initial 12 h exposure to 30 ppm CO, steady-state was reached (35% H_2–D_2 conversion). Regeneration of the catalyst in H_2 for 12 h allowed only a partial recovery of the Pt sites and hydrogen adsorption capacity (ca. 150 μmol H g cat^{-1}). However, the amount of CO-free Pt surface atoms, even after 6 h of regeneration, was enough to allow the H_2–D_2 exchange reaction to achieve equilibrium conversion (~45%). Re-exposure of the regenerated catalyst to 30 ppm CO again resulted in a hydrogen surface concentration similar to that following the initial exposure to CO.

These results suggest that the adsorption/desorption equilibrium of CO on Pt is not affected by whether or not the surface is fresh or pre-poisoned and regenerated. However, while only a partial recovery was again achieved, H_2–D_2 exchange conversion after 6 h regeneration was at equilibrium under the conditions employed.

Therefore, purging with H_2 may appear to initially restore fuel cell performance, but this apparent recovery is not due to the complete removal of CO from the Pt sites. Rather, it appears that there is only a partial recovery of sites—but sufficient CO-free Pt sites are recovered to allow H_2 activation not to be the rate-limiting step any longer. Based on these results, the addition of a H_2 purge between CO exposures may help in slowing its poisoning effect, but it by no means totally reverses this poisoning, unless perhaps if extremely long purge times are used.

4. Conclusions

Comparison of HDSAP results to those of static H_2/CO chemisorption at 80 °C and CO TPD show excellent agreement, thus validating HDSAP as an excellent technique for the measurement of hydrogen surface concentration on Pt in the absence and presence of CO at the experimental conditions employed. While the H_2–D_2 exchange reaction (a model for H_2 activation) is able to reach equilibrium very easily on Pt in the absence of CO, introduction of CO is able to shift the reaction away from equilibrium. This shift from reaction equilibrium is supported by the increase in apparent activation energy of H_2–D_2 exchange from 4.5–5.3 kcal mole^{-1} [24,25] (in the absence of CO) to 19.3–19.7 kcal mole^{-1} (in the presence of 10–70 ppm CO). Apparent activation energy results, in the presence

of CO, agree well with those reported by Montano et al. [25] within experimental error.

Results from the H_2–D_2 exchange reaction, HDSAP, and TPD show that the catalyst surface is not fully saturated by CO in the presence of as high as 200 ppm CO in H_2 under the experimental conditions used (80 °C and 0.4 atm H_2), which suggest that surface coverage estimations via cyclic voltammetry (CV) are inaccurate. Furthermore, comparisons of hydrogen surface concentration and CO measurements with that of static H_2 chemisorption at 35 °C show a CO surface coverage of ca. 0.44–0.56 ML in 2–200 ppm of CO in H_2, respectively. Surface science results of CO surface coverage obtained via HP STM on Pt(1 1 1) for the range of CO studied were consistently ~0.1 ML higher than the values obtained in this study. However, considering the differences in experimental conditions (i.e., room temperature, in the absence of hydrogen, and single crystal surface), CO surface coverages obtained from HDSAP show good agreement with those obtained from surface science.

Regeneration of Pt/C in H_2, at fuel cell conditions, after exposure to 30 ppm CO shows only a partial recovery of surface Pt sites. However, the amount of CO-free sites available from removal of CO in the gas stream can still be enough to achieve equilibrium conversion for H_2–D_2 exchange. This explains why a complete recovery of performance is observed in a fuel cell—not because all of the surface CO has been removed, but because enough has been removed to make H_2 activation not be the rate-limiting step. In addition, surface coverage of hydrogen and CO results at steady-state appear to imply a limiting effect on hydrogen spillover by CO, perhaps due to CO adsorption at Pt–C interface.

With the establishment of HDSAP as a valid technique for the measurement of hydrogen surface concentration on Pt, future research in this series will explore the effects of Nafion and humidity on H_2 activation and surface coverage on Pt in the presence and absence of CO and other impurities. The eventual goal of this work will be a better understanding of the effects of impurities on H_2 activation and hydrogen surface coverage of a Nafion–Pt/C catalyst at various levels of humidity, similar to those typical in a catalyst layer in a PEMFC.

Acknowledgements

References

[1] M.L. Perry, T.F. Fuller, J. Electrochem. Soc. 149 (2002) S59.
[2] X. Cheng, Z. Shi, N. Glass, L. Zhang, J. Zhang, D. Song, Z.S. Liu, H. Wang, J. Shen, J. Power Sources 165 (2007) 739.
[3] R.J. Bellows, E.P. Marucchi-Soos, D.T. Buckley, Ind. Eng. Chem. Res. 35 (1996) 1235.
[4] S. Jimenez, J. Soler, R.X. Valenzuela, L. Daza, J. Power Sources 151 (2005) 69.
[5] S.R. Longwitz, J. Schnadt, E.K. Vestergaard, R.T. Vang, E. Lægsgaard, I. Stensgaard, H. Brune, F. Besenbacher, J. Phys. Chem. B 108 (2004) 14497.
[6] M. Andersen, M. Johansson, I. Chorkendorff, J. Phys. Chem. B 109 (2005) 10285.
[7] J.C. Davies, R.M. Nielsen, L.B. Thomsen, I. Chorkendorff, A. Logadottir, Z. Lodziana, J.K. Norskov, W.X. Li, B. Hammer, S.R. Longwitz, J. Schnadt, E.K. Vestergaard, R.T. Vang, F. Besenbacher, Fuel Cells (Weinheim, Germany) 4 (2004) 309.
[8] H. Igarashi, T. Fujino, Y. Zhu, H. Uchida, M. Watanabe, Phys. Chem. Chem. Phys. 3 (2001) 306.
[9] D.C. Papageorgopoulos, M. Keijzer, J.B.J. Veldhuis, F.A. de Bruijn, J. Electrochem. Soc. 149 (2002) A1400.
[10] A.J. Bard, L.R. Faulkner, Electrochemical Methods: Fundamentals and Applications, 2nd ed., John Wiley & Sons, New York, 2001.
[11] S.D. Ebbesen, B.L. Mojet, L. Lefferts, J. Catal. 246 (2007) 66.
[12] B. Ren, L. Cui, X.F. Lin, Z.Q. Tian, Chem. Phys. Lett. 376 (2003) 130.
[13] P.N. Ross, P. Stonehart, J. Res. Inst. Catal. Hokkaido Univ. 22 (1974) 22.

[14] F. Coloma, A. Sepulveda-Escribano, F. Rodriguez-Reinoso, J. Catal. 154 (1995) 299.

[15] V. Perrichon, L. Retailleau, P. Bazin, M. Daturi, J.C. Lavalley, Appl. Catal. A 260 (2004) 1.

[16] B.A. Riguetto, S. Damyanova, G. Gouliev, C.M.P. Marques, L. Petrov, J.M.C. Bueno, J. Phys. Chem. B 108 (2004) 5349.

[17] R.L. Jia, C.Y. Wang, S.M. Wang, J. Mater. Sci. 41 (2006) 6881.

[18] Z. Zhou, W. Zhou, S. Wang, G. Wang, L. Jiang, H. Li, G. Sun, Q. Xin, Catal. Today 93–95 (2004) 523.

[19] M. Wang, K.D. Woo, D.K. Kim, Energy Convers. Manage. 47 (2006) 3235.

[20] R.L. Borup, J.R. Davey, F.H. Garzon, D.L. Wood, M.A. Inbody, J. Power Sources 163 (2006) 76.

[21] K.E. Swider, D.R. Rolison, Electrochem. Solid-State Lett. 3 (2000) 4.

[22] E. Antolini, F. Cardellini, E. Giacometti, G. Squadrito, J. Mater. Sci. 37 (2002) 133.

[23] A.D. Leuking, R.T. Yang, Appl. Catal. A 265 (2004) 259.

[24] S.L. Bernasek, G.A. Somorjai, J. Chem. Phys. 62 (1975) 3149.

[25] M. Montano, K. Bratlie, M. Salmeron, G.A. Somorjai, J. Am. Chem. Soc. 198 (2006) 13229.

[26] P. Thostrup, E.K. Vestergaard, T. An, E. Lægsgaard, F. Besenbacher, J. Chem. Phys. 118 (2003) 3724.

[27] G.A. Somorjai, X. Su, K.R. McCrea, K.B. Rider, Top. Catal. 8 (1999) 23.

[28] G.A. Somorjai, Appl. Surf. Sci. 121–122 (1997) 1.

[29] T. Mallat, S. Frauchiger, P.J. Kooyman, M. Schurch, A. Baiker, Catal. Lett. 63 (1999) 121.

[30] G.A. Somorjai, Chem. Rev. 96 (1996) 1223.

[31] G.A. Somorjai, J. Carrazza, Ind. Eng. Chem. Fundam. 25 (1986) 63.

[32] F.A. Uribe, S. Gottesfeld, T.A. Zawodzinski, J. Electrochem. Soc. 149 (2002) 293.